Available online at www.sciencedirect.com
ScienceDirect
Corrosion Science 50 (2008) 1481–1491
CORROSION SCIENCE
www.elsevier.com/locate/corsci

The use of SIMS in quality control and failure analysis of electrodeposited items inspected for hydrogen effects

E. Kossoy [a], Y. Khoptiar [a], C. Cytermann [b], G. Shemesh [a], H. Katz [a], H. Sheinkopf [a], I. Cohen [a], N. Eliaz [c,*]

[a] *Materials Division, Depot 22, Israel Air Force, P.O. Box 02538, Israel*
[b] *Solid-State Institute, Technion – Israel Institute of Technology, Haifa 32000, Israel*
[c] *Biomaterials and Corrosion Laboratory, School of Mechanical Engineering, Tel-Aviv University, Ramat Aviv 69978, Israel*

Received 18 December 2007; accepted 9 January 2008
Available online 16 February 2008

Abstract

In high-strength steels it is often difficult to distinguish between hydrogen embrittlement and various other brittle failure mechanisms. The objective of this work was to develop a sensitive analytical procedure based on secondary ion mass spectrometry (SIMS) that would allow in-service identification of local hydrogen accumulation, either during quality control or during failure analysis of electroplated items. Dynamic SIMS was found useful in identifying when baking of Cd-plated AISI 4340 steel was not carried out, thus potentially leading to hydrogen embrittlement. In all non-baked samples, an increase in the hydrogen signal was found at the Cd/steel interface. In baked samples, either a peak was not observed at the interface, or it was insignificant based on determination of the ratios between the hydrogen signals in the coating, interface and substrate. This reproducible effect was monitored even after 16 months storage in a desiccator. These observations make the procedure practical in suggesting more accurate, reliable and cost effective recommendations for prevention of failures. The main effect of baking was found to be effusion of hydrogen from the interface and the substrate steel into the atmosphere. A mechanism for delayed failure is suggested.

Keywords: A. Steel; B. SIMS; C. Electrodeposited films; C. Hydrogen embrittlement; Failure analysis

1. Introduction

Failure analysis is usually a necessary stage in determining the mechanism/s and cause/s of failure, so that effective corrective actions can be implemented and recurrences of the failure can be eliminated (or, at least, minimized) [1]. It is well known, however, that in the case of high-strength steels it is often difficult to distinguish between various brittle failure mechanisms because similar fracture characteristics may appear in each of them [2]. In particular, it is sometimes nearly impossible to tell apart hydrogen embrittlement (HE) and stress corrosion cracking (SCC) in practical failure situations [3]. Obviously, the recommendations for prevention of failure recurrence would be totally different in each case.

High-strength steels might suffer severe loss of ductility, toughness and strength due to HE [4], resulting in sudden fracture (i.e., delayed failure). The susceptibility of steels to HE increases with tensile strength. The embrittlement can be caused by either external or internal hydrogen. Hydrogen can be introduced into the metal either during fabrication (e.g. during cleaning, pickling, phosphating, electroplating, autocatalytic processes, welding or brazing operations, as a result of lubricant breakdown, etc.) or in service (mainly, due to cathodic protection reactions or corrosion reactions) [5]. Atomic hydrogen is codeposited and absorbed in the metal substrate during electroplating [6,7]. In coating systems with low Faradaic efficiency

* Corresponding author. Tel.: +972 3 640 7384; fax: +972 3 640 7617.
E-mail address: neliaz@eng.tau.ac.il (N. Eliaz).

0010-938X/$ - see front matter © 2008 Elsevier Ltd. All rights reserved.
doi:10.1016/j.corsci.2008.01.016

(FE), hydrogen evolution during electrodeposition is enhanced, thus increasing the likelihood of HE. For example, hard chromium coated items are more prone to HE than those coated with cadmium [2]. Even the high efficiency etch-free (HEEF) hard chromium coating, in which the FE was increased from 15% that is typical of conventional hard chromium to 25%, has been found susceptible to HE [8]. In highly efficient systems, such as Cu and Ag baths, codeposition of hydrogen occurs only when the limiting current density is exceeded, or when the added complexing agents shift the potential of metal deposition to sufficiently negative values. The higher the hydrogen overpotential on a given metal, the lower the amount of hydrogen absorbed in it [6]. One of the mechanisms that have been suggested to explain the HE of steels is the high-pressure bubble formation [4]. Eliaz et al. [9] have recently developed a coupled diffusion/fracture mechanics approach to describe the expansion of high-pressure hydrogen bubbles and propagation of cracks between them in the absence of external loads, allowing determination of the time to failure.

Heat treatment (“baking”) is commonly employed following electroplating of various coatings in order to render the normally mobile hydrogen immobile. For high-strength steels electrodeposited with hard chromium, for example, this is typically done at 177–205°C for at least 3 h. The treatment is required for all steel parts hardened to 40 R_C or more, and should be applied not later than 4 h after the completion of the plating process [10]. Evaluation of the effect of residual hydrogen on the mechanical properties is then done according to standards such as ASTM F 519 [11] and ASTM F 1624 [12]. Certain very susceptible alloys require the use of fabrication processes other than electroplating.

Although hydrogen diffusion is exponentially increased with temperature, the required time to reduce the diffusible hydrogen concentration to a given level increases with the square of the section thickness. For thick sections this can mean hundreds of hours at any common baking temperature. Even then, there is no guarantee that permanent damage or irreversible HE has not already occurred [2]. In the case of Cd plating, for example, the high solubility of hydrogen in Cd relative to that in the iron-based substrate makes the Cd-layer a source during the initial stage of baking; consequently, the hydrogen concentration in the steel substrate may increase [13]. Moreover, because the diffusivity of hydrogen in Cd is much lower than that in steel, the Cd-layer acts as a diffusion barrier to outgasing of hydrogen during baking, and a significant concentration of dissolved hydrogen might remain in the steel, even after baking times of 100 h [14].

If standard procedures are followed precisely, HE-related failures of electroplated items can usually be prevented. However, if improper baking process was carried out, or such a treatment was not carried at all, delayed failure might occur. In many practical cases of in-service failures, even when a failed item is suspected for HE, it is not easy to confirm whether all manufacturing processes were carried out properly. Then, in order to prevent failures of items from the same manufacturing batch, there is often no choice but to remove the entire batch from service. This solution is usually complicated and costly, in particular when considering critical aeronautical components. Furthermore, taking into account that random hydrogen charging often cannot be eliminated or easily controlled by platers, testing representative quantities of the finished items is necessary in the framework of quality control [5]. Hence, an accurate, sensitive experimental procedure that is capable of mapping the level of residual hydrogen would be very useful both at the stage of quality control and at the stage of failure analysis. This was the goal of the present work. Because high-strength steels might be embrittled even by very low concentrations of hydrogen, and because the ability to reach locally a critical concentration of hydrogen is more significant than the mean concentration of hydrogen in the bulk of the metal, local hydrogen quantification is necessary for practical evaluation of the risk of HE. Experimental methods such as the hydrogen microprint technique [15,16], tritium autoradiography [17,18] and thermal desorption spectroscopy (TDS) [19] were evaluated and found unsuitable to accomplish this project’s goal.

In secondary ion mass spectrometry (SIMS), a solid sample material is bombarded with a focused primary ion beam (300 eV–30 keV). The primary ions are implanted into the sample down to tens of nm. A transfer of kinetic energy takes place between the surface atoms and collision cascades are created. Some collisions are oriented backwards toward the surface. If they have enough energy to overcome the surface barrier potential, atoms, molecules and molecular fragments are ejected (sputtered) from the sample surface. Most of these particles are neutrals, but a small fraction is ionized, either positively or negatively. These secondary ions, characteristic of the composition of the analyzed volume, are separated according to their mass-to-charge ratio and collected. SIMS combines simultaneous detection of ions over a virtually unlimited mass range (from hydrogen to uranium), at high mass resolution (up to 0.02 amu), at sensitivities that may be as high as ppb-ppm, with mapping of the lateral distribution of species and with depth profiling. Its drawbacks include the requirement for UHV-compatible and size-limited samples, a very high sensitivity for surface morphology and surface contaminants, typically limited optical capabilities that make it difficult to find grains or local regions of interest for analysis, the need for an expert operator, and a relatively high cost [20].

There are two major types of SIMS instruments: static and dynamic. In static SIMS, a very low ion beam current density is used and less than 1% of the original surface of the sample is consumed during the course of the analysis. Its time-of-flight (TOF) mass analyzer separates the ions at a field-free drift path according to their kinetic energy. The analysis and the sputtering (if conducted) are con-

ducted separately. The spatial resolution is ~0.1 μm (imaging), the depth resolution is several angstroms and, because of the small primary intensities used, the sputtering depth is usually limited to ~1μm. Static SIMS can suggest molecular structures and observe extremely high mass fragments (e.g. of polymers), which dynamic SIMS cannot do. In dynamic SIMS, a much higher primary ion beam current density is used. The surface of the sample is continuously etched away during the course of the analysis. A quadrupole or magnetic sector mass analyzer separates the masses, where only masses of choice are able to pass. The spatial resolution is a few micrometers (imaging), the depth resolution is a few nanometers (depending on the primary ion energy), and a sputtering depth of tens of micrometers is possible [20].

SIMS has already been applied to a limited extent in mechanistic investigations of HE and SCC, with some success, as well as to identify the traps for hydrogen isotopes in different alloys. Takai et al. [21,22] used SIMS to visualize the trapping sites of deuterium in high-strength steels. Line scans showed that the concentration of deuterium at inclusions, grain boundaries, and phosphorous segregation bands in a steel bar for prestressed concrete was 11.0, 7.8 and 5.0 times higher than that in the matrix, respectively. Fractured samples were analyzed following FIP test for hydrogen-induced SCC. Based on TDS analysis it was concluded that it is necessary to promptly carry out SIMS analysis of the trapped deuterium, either around inclusions or at the grain boundaries, within 24 h after the delayed fracture test, otherwise the measured signal would be too low [21]. Later [23], these authors combined SIMS with TDS in order to visualize the initial deuterium distributions in a spheroidal graphite cast iron, and to relate the desorption profiles during different heat treatments with trapping sites. Deuterium was used instead of hydrogen as the detected ion in order to increase the sensitivity. Brass et al. [24] performed tritium autoradiography and deuterium profiling by SIMS on pre-cracked and then bolt-loaded double cantilever beam (DCB) specimens made of 4120 HSLA steel in order to measure the hydrogen concentration in the plastic zone at the crack tip. The samples were cathodically charged, repolished and quenched at −196°C in order to prevent deuterium desorption. A three orders of magnitude drop in the deuterium concentration was observed after 100 h aging at 20°C. Next, Chene et al. [25] introduced deuterium into flat tensile specimens made of Ni-based alloy 600 by potentiostatic cathodic polarization. SIMS profiles were calibrated by thermal extraction of deuterium and correlated to fracture surfaces in order to assess the effect of deuterium concentration on the extent of intergranular fracture pattern. Sastri and McDonnell [26] applied the hot-extraction thermal conductivity method, SIMS, anodic dissolution, and the reaction of the liberated hydrogen with nitroxyl free radical method, in the determination of surface enriched hydrogen in AISI 1062 and 4037 steels. The results supported the hypothesis that HE originates in the thin outer surface layers of these steels. Mao and Li [27] used SIMS to measure the hydrogen distribution around a crack tip in compact tensile (CT) specimens made of pipeline steel X-80. These specimens had been loaded by a wedge and subjected for 72 h to SCC. The results indicated generation and accumulation of hydrogen around the SCC crack tip. Shvachko [28] used the SIMS to investigate the hydrogen state on pure iron pre-charged electrolytically with hydrogen. It was found that the ability to measure negative ion emission extends the analytical capability of SIMS in the investigation of Fe–H interaction phenomena, and that the hydrogen atoms diffusing from the bulk of iron can bear a negative charge on its surface.

None of references [21–28] deals with, or is directly related to, electroplating, baking, quality control and failure analysis of real, engineering parts. They all involved analysis of deuterium (instead of hydrogen), polished samples, quenching at cryogenic temperatures to prevent hydrogen desorption before SIMS analysis, or performance of the SIMS analysis quickly after the hydrogen was introduced into the material and/or delayed failure occurred. These characteristics, in addition to the use of specimens that are not always easy to extract from in-service parts, make them less useful for the type of tasks of interest in this study. Therefore, the objective of the present research was to develop an in-service analytical procedure based on SIMS that would allow identification of local hydrogen accumulation either during quality control or during failure analysis of electroplated items. This procedure should be helpful in distinguishing between HE and other possible failure mechanisms in high-strength steels. Availability of such a method would give way to more accurate, reliable and cost effective recommendations for the prevention of failure recurrence. It could also be used in courts, when the aptness of the baking process is questioned. To the best of the authors' knowledge, such use of SIMS has not been reported before elsewhere.

For this work, AISI 4340 low alloy steel was selected. This steel combines deep hardenability with high ductility, toughness and strength. It is typically used in heavy-duty structural parts, such as aircraft landing gears, power transmission gears and shafts, etc. This steel becomes susceptible to HE when heat treated to tensile strengths above 1400 MPa (200 kpsi). Hence, parts exposed to hydrogen during manufacturing are usually baked subsequently. In addition, this steel exhibits extremely poor resistance to SCC when tempered to tensile strengths of 1500–1950 MPa (220–280 kpsi).

2. Experimental procedures

2.1. Dynamic SIMS analyses

At an early stage of the project, samples were analyzed by static SIMS. However, due to several limitations that were identified, it was eventually decided to focus on dynamic SIMS.

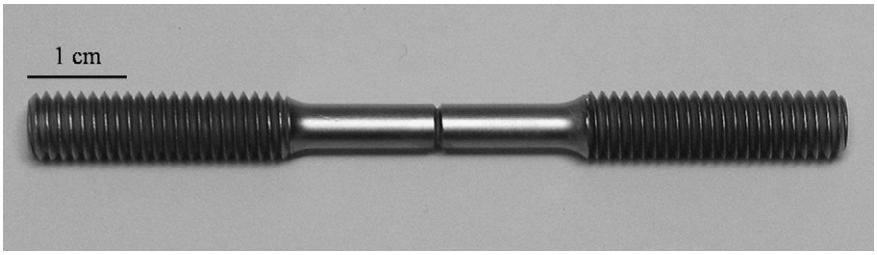

Fig. 1. A standard [10] tensile V-notch (TVN) sample made of AISI 4340 steel heat treated to 50–53 R_C.

2.1.1. Instrument specifications, calibration and operating conditions

A Cameca ims 4f dynamic SIMS instrument was used. A 18–25 nA, 5.5 keV Cs^+ primary ion beam was rastered over a sputtering square area that varied between 50×50 μm and 250×250 μm, while the analyzed area was set to 33 μm (in diameter) at the center of the crater. The secondary negative ions H^-, Fe^-, C^-, O^- and CdO^- were monitored. The CdO^- secondary ions was preferred over Cd^- because the latter has a very low secondary yield. The samples were biased at −4.5 kV. The choice of H^- is related to its higher sensitivity in SIMS. The samples were introduced into the SIMS chamber at least 12 h before the measurement in order to minimize the environment contribution to the hydrogen secondary yield. The base pressure before analysis was 2×10^{-10} Torr. The resulting crater depths were measured with the aid of a depth profilometer (model Tencor 200), with a precision of 5%.

An attempt was made to calibrate the instrument for quantitative analyses of the hydrogen concentration. In addition, the sputtering rate was determined for the AISI 4340 steel. To these aims, a sample with dimensions of $7 \times 12 \times 5$ mm was cut from a steel bar hardened to 50–53 R_C. The sample was polished in a water-based alumina suspension to 0.05 μm, cleaned ultrasonically in 2-propanol for 1 min, air dried, and stored in a desiccator. Next, hydrogen ions implantation was carried out into 2/3 of the area, at a dose of 10^{15} atoms/cm^2 and ions energy of 40 keV. Computer simulation predicted that under these conditions, a maximum hydrogen concentration of 7×10^{19} atoms/cm^3 would be established at a depth of 216 ± 61 nm. After ions implantation, the specimen was kept in liquid nitrogen until the SIMS analysis began. That analysis, however, did not reveal any difference in the hydrogen concentration within the implanted and non-implanted areas. This could be either due to a high background contribution from hydrogen in the vacuum chamber or, more likely, due to rapid desorption of hydrogen into the vacuum phase (the equation of diffusion length may be used to estimate the time required for the escape of hydrogen from the thin ion-implanted layer). By measuring the crater depth after sputtering, the typical sputtering rate was determined. Thus, it was found that the sputtering rate was increased from 0.18 nm/s to 1.2 nm/s and then to 3.2 nm/s as the sputtering area was reduced from 250×250 μm to 100×100 μm and then to 50×50 μm, respectively.

2.1.2. Analysis of a fracture surface

Since local accumulation of hydrogen generally leads to failure initiation by intergranular cracking (IGC), a correlation was sought between the local hydrogen signal and the fracture pattern at that analysis point. A standard [11] tensile V-notch (TVN) specimen (Fig. 1), heat treated to hardness of 50–53 R_C, was electroplated with Cr in accordance with QQ-C-320 [10]. No baking was performed afterwards. The reason for selecting Cr and not Cd was to maximize the effect of hydrogen on the mechanical properties and fracture mode. When the specimen was loaded statically to 77% of the steel ultimate tensile strength, it fractured within a few seconds. Two cylindrical samples, each approximately 1 cm long and containing one of the opposing fracture surfaces, were cut. The fracture surface was first examined under a stereoscope. Next, one fracture surface was analyzed using a Scanning Electron Microscope (Jeol JSM-7000F Field-Emission SEM). The other sample was cleaned ultrasonically for 1 min in 2-propanol, air dried, and kept in a desiccator for 46 days before SIMS analysis was carried out. This long storage period after fracture was chosen as to mimic real failure analysis events. The depths of measurement were between 3.1 and 4.5 μm.

2.1.3. Analyses through Cd plating

A second approach was to measure hydrogen depth profiles during sputtering through a Cd electroplate into the substrate steel. Since the electroplating protects the metal surface from contamination and prevents outgassing of hydrogen, this approach was expected to provide more reliable results. It may be useful both in quality control and in failure analysis, for instance by acquiring depth profiles close and in parallel to the fracture surface. A comparison was made between baked and non-baked samples.

Two rectangular samples were prepared from steel hardened to 40–42 R_C. The samples were ground on a 120-grit paper and cleaned ultrasonically for 1 min in 2-propanol. Following cleaning in an alkaline bath, cadmium electroplating was applied for 1.5 min, in accordance with QQ-P-416, type I, class 3 [29]. One sample, designated herein as B1, was immediately baked at 191°C for 23 h. The other sample, designated herein as NB1, was not baked. The

thickness of the coating was measured on metallographic cross-sections by means of a Reichart–Jung MeF-3 light microscope. It was found to be 5 μm. The remaining parts of the two samples, about $6 \times 6.5 \times 4$ mm each, were cleaned ultrasonically for 1 min in 2-propanol, air dried, and kept in a desiccator until SIMS analysis started. Overall, nine days passed from electroplating to measurement. The sputtering area was 250×250 μm, whereas the depths of measurement were between 5.0 and 9.5 μm.

In order to demonstrate reproducibility, seven $9 \times 6 \times 4.5$ mm samples were prepared as described above, except for increasing the plating time to 4 min. Three samples, designated herein as B2, B3 and B4, were immediately baked at 191°C for 24 h. Three samples, designated herein as NB2, NB3 and NB4 were not baked. The seventh sample was not baked, but served for measuring the coating thickness. The latter was found to be 10–15 μm. The six samples for SIMS analysis were stored in a desiccator for 56 d before SIMS analysis. SIMS depth profiles were acquired at three different points on each sample. In each measurement, which lasted about 20 min, the primary ion beam current was 20 nA, the analyzed area was 33 μm in diameter, and the sputtering area was 125×125 μm. The measurements were terminated when all signals became stable, within the bulk of the steel.

Finally, in order to confirm whether any observed phenomenon can be identified even after extremely long periods, simulating the worse scenario in real-life failure analyses, two Cd-coated samples were arbitrarily chosen and reanalyzed after 16 months storage in a desiccator. One sample (designated herein as B5) was originally baked immediately after electroplating, while the other one (designated herein as NB5) was not.

3. Results and discussion

3.1. Analysis of a fracture surface

The high-strength TVN specimen that was electroplated with Cr without performing subsequent baking (see Section 2.1.2) exhibited a brittle failure mode. Fractography (Fig. 2) revealed two distinct regions. A peripheral

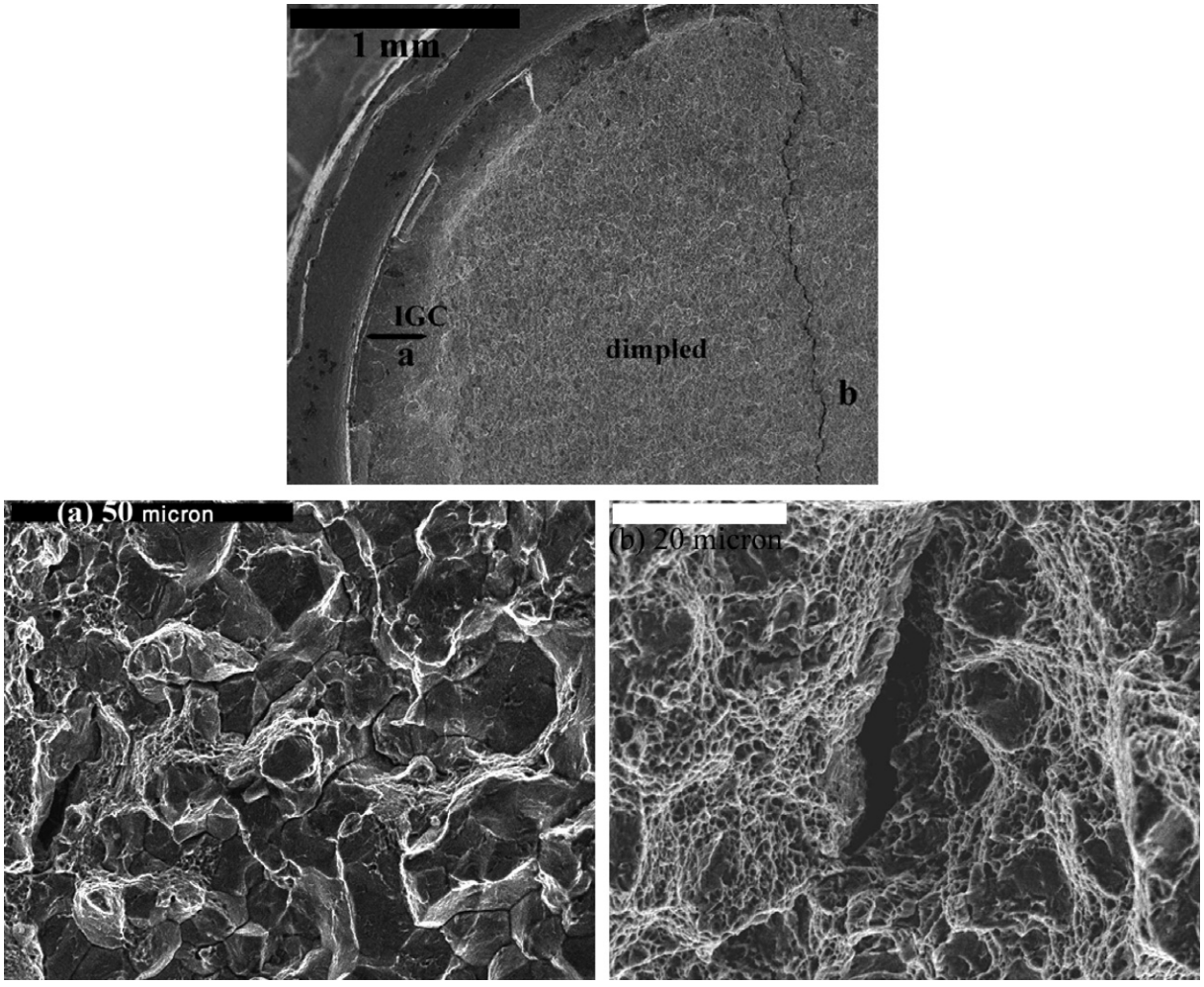

Fig. 2. SEM images of the fracture surface of a Cr-plated, non-baked TVN sample, fractured at 77% of the ultimate tensile strength. The fracture surface consists of a peripheral intergranular region (a) and an inner dimpled (overload) region (b).

intergranular fracture surface was found to exist along roughly half of the perimeter, penetrating approximately 120 μm into the sample. Such an intergranular pattern along prior austenite grain boundaries is typical in failures of high-strength steels due to HE. The rest of the fracture was characterized by a dimpled rupture, typical of a failure by overload, with randomly oriented 50–100 μm long cracks.

SIMS analyses were made at four points, two within the IG region and two at the center of the dimpled area. Note that the size of grains, which varied between 10 and 30 μm, was comparable with the analyzed area (33 μm in diameter). No correlation between the intensity of the hydrogen signal and the fracture pattern was observed. The reasons for this inability to map a hydrogen-enriched region may be: (1) A rapid escape of hydrogen from the fracture surface due to its high diffusivity in the steel, (2) the high roughness of (any) fracture surface, (3) adsorption of contaminants on the fracture surface, masking the hydrogen effect, and (4) a too high hydrogen background signal. Thus, it was decided to evaluate an alternative approach for identifying the residual hydrogen.

3.2. Analysis through Cd plating

In contrast to the results discussed so far, hydrogen depth profiles through the Cd plating revealed clear differences between the baked and the non-baked samples. Typical logarithmic plots of the secondary ion yields as a function of time are presented in Figs. 3a and b for the baked and non-baked samples, respectively. It should be noted that the sputter rate in the Cd plating is much higher than in the underneath steel. Therefore, to plot the secondary ion yield as a function of depth would have required a careful point weighted calculation of the sputter rate at the Cd/steel interface. In addition, in order to compare between the measurements, the profiles were normalized by the average Fe^- intensity in the steel. A sharp Cd/steel interface can easily be distinguished in Fig. 3, despite the roughly ground (namely, 120 grit) surface. The interface is characterized by a decrease in the signal of CdO^- and an increase in the signals of Fe^- and C^-, when penetrating into the steel substrate. Thus, it may be concluded that SIMS depth profiles of CdO^-, Fe^- and C^- may be used to identify the Cd/steel interface. The initial decrease in the hydrogen ion signal (as well as in other ion signals) may be attributed to the implantation and accumulation of Cs^+ ions from the sputtering ion beam, until saturation is attained. It has already been reported that, while being accumulated in the sample, Cs^+ ions may affect the extent to which surface atoms are ionized [21].

The most important observation in this study was that the hydrogen signal was increased at the Cd/steel interface in all non-baked samples. This phenomenon is illustrated in Fig. 3c, in which the intensity is drawn on a linear scale. Comparison of the hydrogen profiles for the baked and for the non-baked samples enabled to exclude the attribution of variation in the hydrogen level to changes in the hydrogen ionization yield in different media (namely, steel versus Cd). Thus, a simple depth profile through the plating may aid in determining when HE due to internal hydrogen might become a concern in an electroplated item. SIMS may be a very sensitive and reliable technique for identifying when baking was not done at all, or was done improperly. From the fracture pattern shown in Fig. 2 it could be estimated that hydrogen accumulation and damage was most significant around the coating/steel interface, where intergranular fracture pattern was observed. Results from tensile tests, either sustained load tests or incremental step load tests, have been used before also by other researchers to indirectly support the mechanism according to which baking after plating allows the atomic hydrogen to be removed and effuse through the coating and also be more homogeneously distributed in the bulk of the substrate metal. Paatsch and Hodoroaba [30] have applied the glow discharge emission optical spectroscopy (GD-OES) technique and showed that hydrogen depth profiles may be used to distinguish between baked and non-baked samples in systems such as Zn on steel, Cd on steel and Co–Pt–W on Cu [30]. The exact concentration of hydrogen could not be determined in that study.

Four questions may be raised at this stage: (1) Is the aforementioned effect observed by SIMS in non-baked samples reproducible? (2) May it appear also in properly baked samples? (3) How sensitive is it to the location of SIMS measurement along the sample? (4) Is it possible to observe it even after longer storage periods? In order to answer questions (1) through (3), six more samples were analyzed – three with baking and three without (see Section 2.1.3). SIMS depth profiles were recorded at three different positions in each sample. In all measurements, a peak in the signal of hydrogen was observed at the Cd/steel interface in non-baked samples. This is demonstrated in Fig. 4c for sample NB3. Therefore, it may be concluded that the detected effect seems to be reproducible. Of course, it is advisable to carry out more experiments in order to increase the population and provide a proper statistical analysis.

A short explanation of the hydrogen background should be provided at this stage. The hydrogen background increases as either the raster size is increased or the sputtering rate is decreased. Hence, the background for all samples presented in Fig. 4 must be relatively low. The background is different in Cd and in steel because of the difference in sputtering rate (in the Cd-layer it is unlikely to be high because of the high sputtering rate for Cd). This was confirmed in baked samples, in which a decrease of the raster size from 150 to 50 μm did not result in further decrease in the hydrogen signal in the steel substrate. The implication of this observation is that the hydrogen signal in the steel is meaningful at a raster size of 125 μm, which was used when acquiring the profiles presented in Fig. 4.

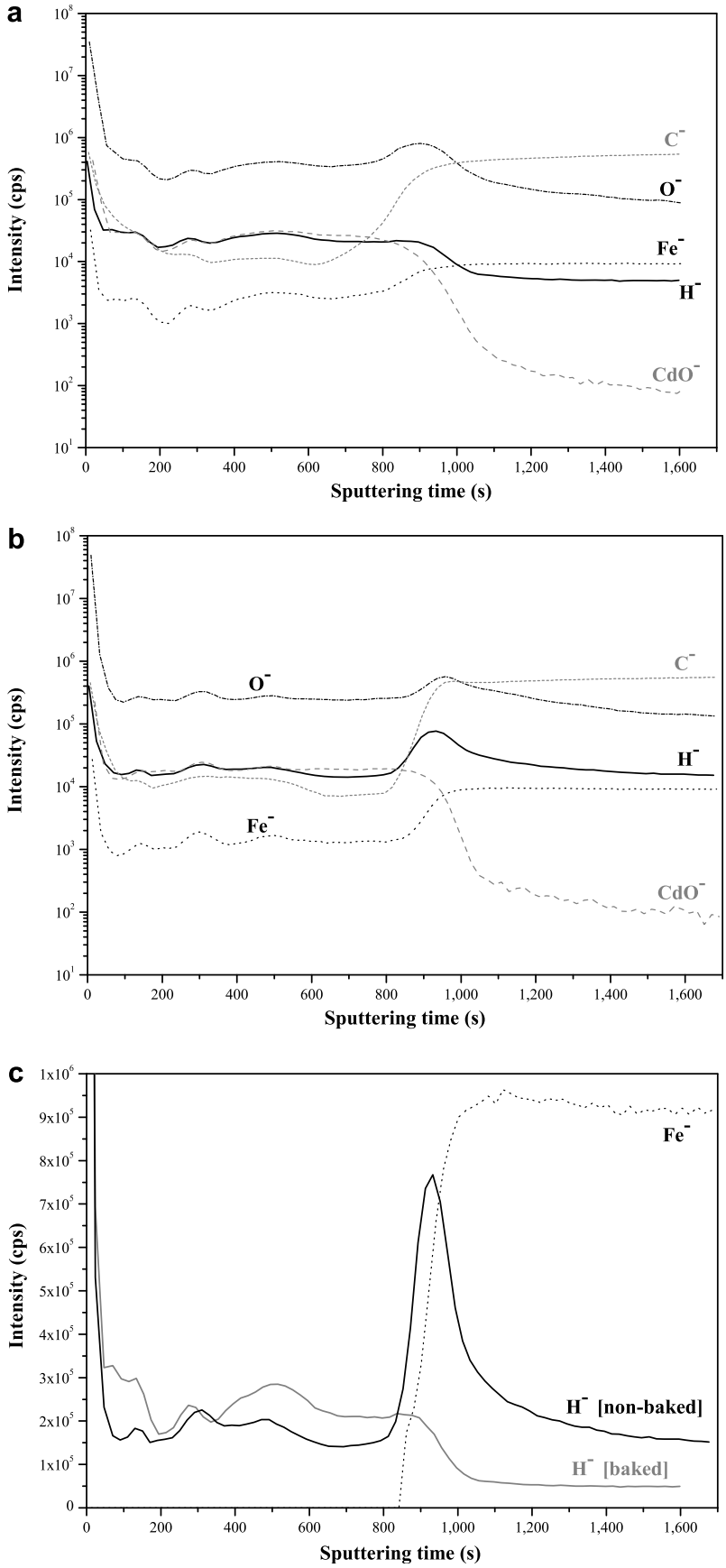

Fig. 3. Typical dynamic SIMS depth profiles measured across the Cd plating in: (a) a baked sample, (b) a non-baked sample, and (c) comparison of typical hydrogen depth profiles in baked and in non-baked samples, with the intensity being drawn on a linear scale.

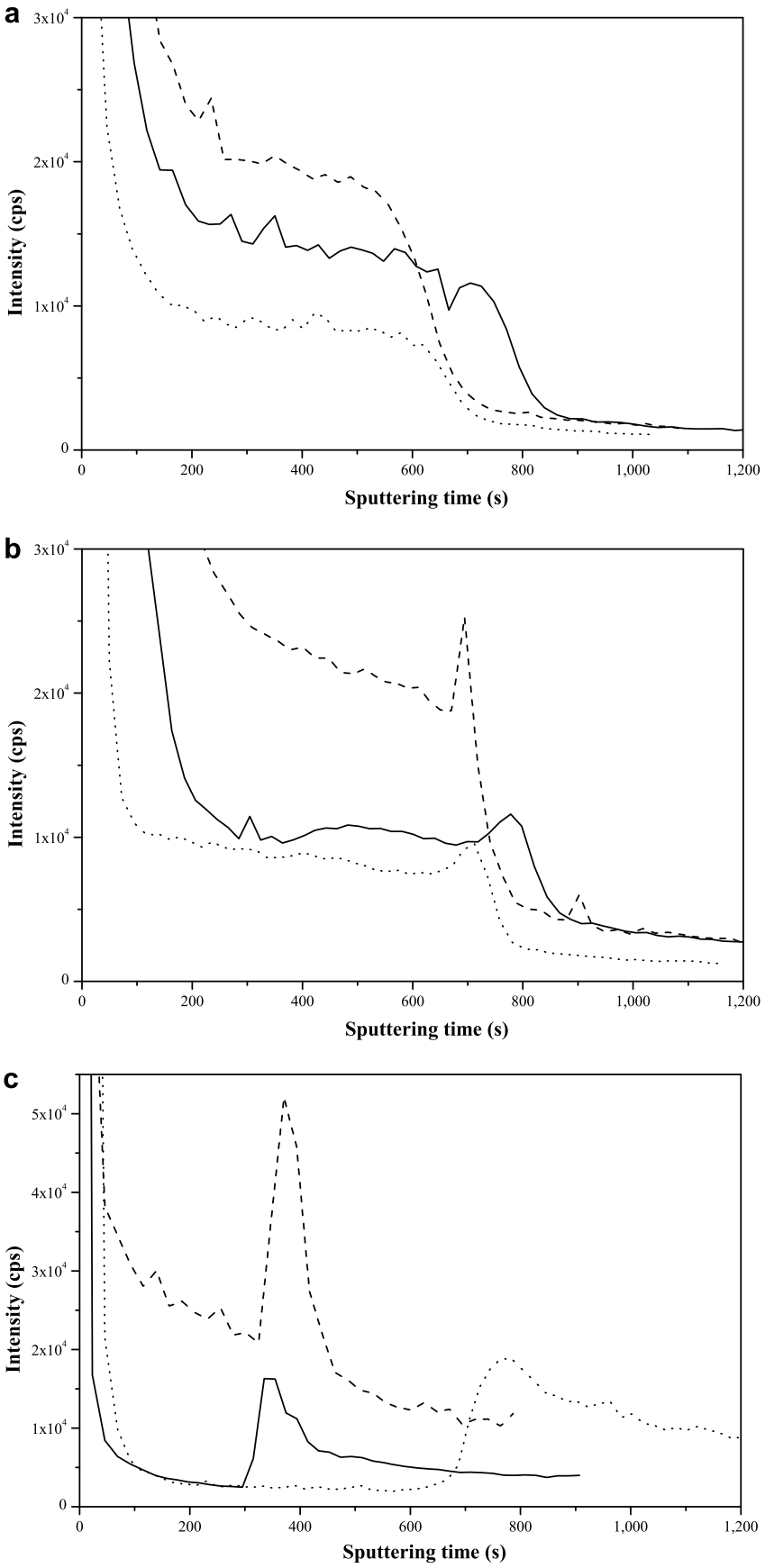

Fig. 4. Hydrogen (H^-) depth profiles obtained from two baked (a–b) and one non-baked (c) samples. In each sample, the profile was acquired at three different regions.

Table 1
Quantitative characteristics of the H^- depth profiles in baked (B) and non-baked (NB) Cd-plated samples

Sample name–number of measurement	$H^-_{interface}/H^-_{coating}$	$H^-_{steel}/H^-_{coating}$	$H^-_{interface}/H^-_{steel}$
B2–1	1.00	0.125	8.00
B2–2	1.28	0.170	7.53
B2–3	1.20	0.175	6.86
B3–1	1.00	0.107	9.35
B3–2	1.00	0.085	11.76
B3–3	1.00	0.132	7.58
B4–1	1.38	0.519	2.66
B4–2	1.00	0.066	15.15
B4–3	1.50	0.300	5.00
NB2–1	2.59	1.310	1.98
NB2–2	3.11	0.791	3.93
NB2–3	2.53	0.683	3.70
NB3–1	6.54	1.610	4.06
NB3–2	2.50	0.570	4.39
NB3–3	9.45	4.450	2.12
NB4–1	4.70	2.090	2.25
NB4–2	2.51	0.807	3.11
NB4-3	4.30	1.500	2.87

$H^-_{interface}$ is the strongest signal detected at the Cd/steel interface; $H^-_{coating}$ is the weakest signal within the coating layer, closest to the interface; H^-_{steel} is the signal at the deepest point analyzed within the substrate steel.

Referring to question (2), nine hydrogen depth profiles were recorded from samples B2–B4. In five of these, no hydrogen peak was observed at the Cd/Steel interface [see, for example, Fig. 4a for sample B3]. However, in the remaining four profiles, a small hydrogen peak was observed at the interface [see Fig. 4b for sample B2]. Fortunately, a complementary quantitative analysis can be suggested (see below) in order to prevent an unambiguous interpretation of SIMS data. To the best of our knowledge, this is the first time ever that such an analysis is proposed.

Table 1 summarizes three quantitative characteristics of the H^- depth profiles in baked and non-baked Cd-plated samples, namely the $H^-_{interface}/H^-_{coating}$, $H^-_{steel}/H^-_{coating}$ and $H^-_{interface}/H^-_{steel}$ ratios. Here, $H^-_{interface}$ is the strongest signal detected at the Cd/steel interface, $H^-_{coating}$ is the weakest signal within the coating layer – closest to the interface, and H^-_{steel} is the signal at the deepest point analyzed within the substrate steel. In all cases, the depths of measurement were between 6.14 and 9.63 μm. The values below are presented in terms of (mean ± standard error). From Table 1 it is evident that while the $H^-_{interface}/H^-_{coating}$ ratio was 1.00–1.50 (1.15 ± 0.07) in the baked samples, it increased to 2.50–9.45 (4.25 ± 0.80) in the non-baked samples. In addition, while the $H^-_{steel}/H^-_{coating}$ ratio was 0.066–0.519 (0.19 ± 0.05) in the baked samples, it increased to 0.570–4.450 (1.53 ± 0.40) in the non-baked samples. Finally, while the $H^-_{interface}/H^-_{steel}$ was 2.66–15.15 (8.21 ± 1.21) in the baked samples, it reduced to 1.98–4.39 (3.16 ± 0.30) in the non-baked samples. In order to determine whether the differences between the means for the baked and for the non-baked samples are statistically significant, a Student's t-test was performed, using Microsoft Excel software. For a probability level $p = 0.05$ (i.e. 95% probability of making a correct statement) and 16 degrees of freedom ($n_1 + n_2 - 2$), the tabulated t-value equals 2.12. The calculated t-values were 3.88, 3.33 and 4.04 for $H^-_{interface}/H^-_{coating}$, $H^-_{steel}/H^-_{coating}$ and $H^-_{interface}/H^-_{steel}$, respectively. Because all three calculated t-values are higher than the tabulated value, it may be concluded that the means are significantly different for the baked and for the non-baked samples. Thus, it may be concluded that baking resulted in a significant decrease in the concentration of hydrogen in the steel compared to its concentration in the Cd coating. In addition, while following baking the Cd/steel interface became less enriched in hydrogen compared to the Cd coating itself, the steel substrate became less enriched in hydrogen compared to the interface. This suggests that the main effect of baking was effusion of hydrogen from the substrate steel and the Cd/steel interface, through the coating, into the atmosphere. Yet, it cannot be excluded that homogenization of hydrogen distribution within the bulk of the substrate steel also occurred to some extent as a result of hydrogen diffusion from the interface zone deeper into the steel, where SIMS analysis was not carried out.

It is important to mention that both the iron and the oxygen depth profiles did not differ between the baked and the non-baked samples. Thus, it can be concluded that the changes in the intensity of the hydrogen signal reflected changes in the amount of hydrogen, rather than changes in its ionization yield due to changes in the yield of other ions. Furthermore, referring to question (3) above, it seems that the same effect may be identified at different locations along the surface of the samples; so, it does not limit the investigator to a specific zone, which might be more difficult to track in real in-service failure analyses.

Finally, referring to question (4), two samples – one baked and one non-based – were reanalyzed by dynamic SIMS 16 months after plating. Remarkably, in contrast to all previous publications (see, for example, Refs. [21,24]), a similar effect was monitored, as evident in Fig. 5. This finding has two important implications. Firstly, it indicates that HE-related delayed failures of improperly baked electroplated items may be related to the time-independent accumulation of hydrogen at the coating/substrate interface, and not necessarily to irreversible damage that occurred in the substrate metal during fabrication – as usually claimed in the literature. Depending on the concentration of hydrogen at the interface, blistering and delamination might occur, or the interface may serve as a reversible hydrogen trap that provides a reservoir of diffusible (mobile) hydrogen for the steel. In the latter case, in an event that energy is absorbed in the material which is sufficient to overcome the activation energy barrier for hydrogen detrapping from the interface, so that diffusion of hydrogen towards strong irreversible traps in the steel is enhanced, the base metal itself may become embrittled within its bulk. Secondly, it seems that there is no time con-

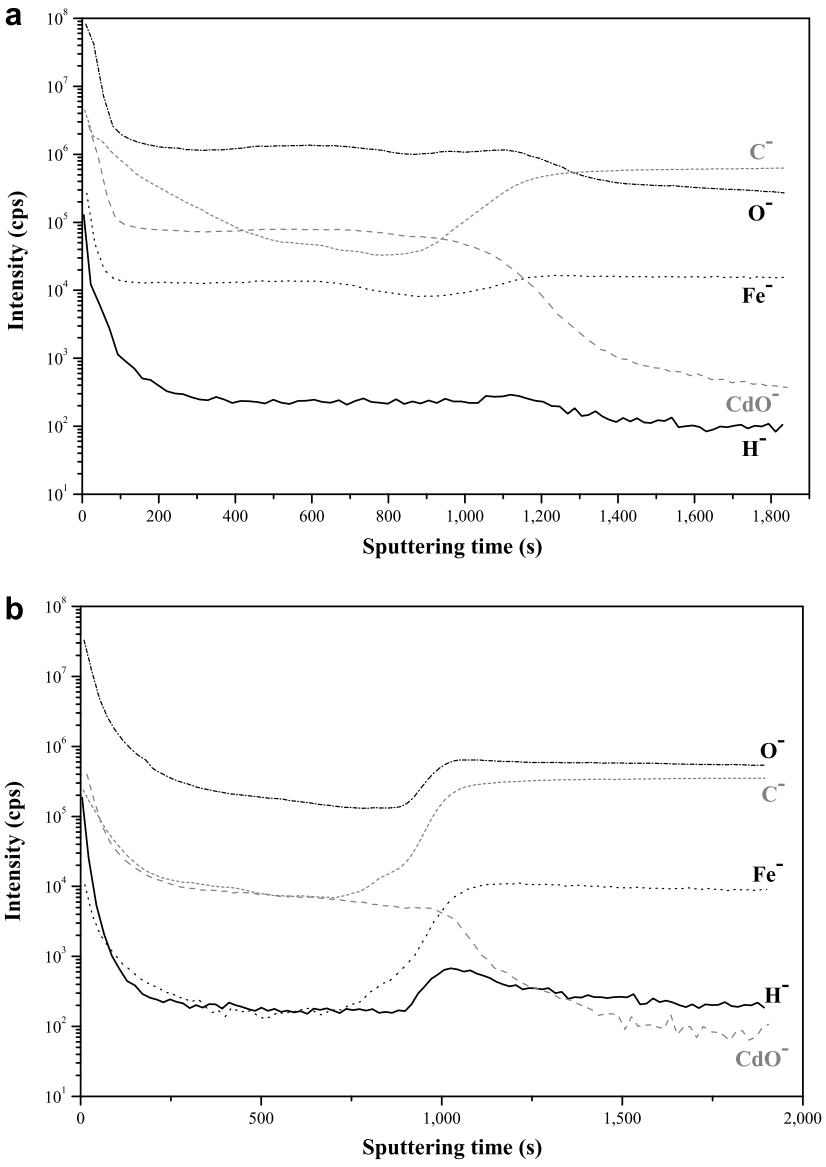

Fig. 5. Typical dynamic SIMS depth profiles measured after 16 months storage in a desiccator across the Cd plating in: (a) a baked sample and (b) a non-baked sample.

straint for the use of SIMS analyses in failure analyses of electroplated items suspected for hydrogen damage.

4. Conclusions

This paper demonstrated the effectiveness of dynamic SIMS in recognizing improper baking of Cd-electroplated AISI 4340 steel, which resulted in hydrogen embrittlement. The following conclusions may be drawn:

(1) In non-baked samples, an increase in the hydrogen signal is found at the Cd/steel interface. In baked samples, either a peak is not observed at the interface, or it could be ignored based on determination of the ratios between the hydrogen signals in the coating, interface and substrate.
(2) The main effect of baking seems to be effusion of hydrogen from the interface and the substrate steel into the atmosphere.
(3) The reproducible effect can be monitored even after very long storage times (e.g. 16 months storage in a desiccator).
(4) HE-related delayed failures may be explained in terms of the time-independent reservoir of hydrogen at the coating/substrate interface, rather than in terms of irreversible damage that occurred within the substrate during electroplating.
(5) The suggested procedure may be used either during quality control or during failure analysis of electroplated items. It should be practical in suggesting more accurate, reliable and cost effective recommendations for prevention of failures (e.g. by distinguishing between HE- and SCC-related failures).

Acknowledgements

The authors are grateful for the financial support of the Israel Ministry of Defense. The authors thank A. Gladkich for conducting the static SIMS tests.

References

[1] N. Eliaz, R.M. Latanision, Preventative maintenance and failure analysis of aircraft components, Corros. Rev. 25 (2007) 107–144.
[2] N. Eliaz, A. Shachar, B. Tal, D. Eliezer, Characteristics of hydrogen embrittlement, stress corrosion cracking and tempered martensite embrittlement in high-strength steels, Eng. Fail. Anal. 9 (2002) 167–184.
[3] ASM Committee on Use of Fractography for Failure Analysis, Metals Handbook, Fractography and Atlas of Fractographs, eighth ed., vol. 9, ASM, Ohio, 1974, p. 111.
[4] H.G. Nelson, Hydrogen embrittlement, in: C.L. Briant, S.K. Banerji (Eds.), Treatise on Materials Science and Technology, vol. 25, Academic Press, New York, 1983, pp. 275–359.
[5] ASTM B 839 – 94, Standard test method for residual embrittlement in metallic coated, externally threaded articles, fasteners, and rod – inclined wedge method, ASTM, West Conshohocken, 1994.
[6] N. Eliaz, E. Gileadi, Induced codeposition of alloys of tungsten, molybdenum and rhenium with transition metals, in: C.G. Vayenas, R.E. White (Eds.), Modern Aspects of Electrochemistry, vol. 42, Springer-Verlag, New York, 2008.
[7] J.W. Dini, Electrodeposition: The Materials Science of Coatings and Substrates, Noyes Publications, New Jersey, 1993.
[8] N. Eliaz, Comparison between the conventional and high-efficiency hard chromium platings in regard to aeronautical demands, J. Adv. Mater. 34 (2001) 27–34.
[9] N. Eliaz, L. Banks-Sills, D. Ashkenazi, R. Eliasi, Modeling failure of metallic glasses due to hydrogen embrittlement in the absence of external loads, Acta Mater. 52 (2004) 93–105.
[10] QQ-C-320, Chromium plating (electrodeposited), Federal Specification, 1987.
[11] ASTM F 519 – 93, Standard test method for mechanical hydrogen embrittlement evaluation of plating processes and service environments, ASTM, West Conshohocken, 1993.
[12] ASTM F 1624 – 95, Standard test method for measurement of hydrogen embrittlement in steel by the incremental loading technique, ASTM, West Conshohocken, 1995.
[13] D.A. Berman, The effect of baking and stress on hydrogen content of cadmium plated high strength steels, Mater. Perf. 24 (1985) 36–41.
[14] J.B. Boodey, V.S. Agarwala, Hydrogen in Metals: Cadmium Plated Steels, Corrosion 87, NACE, Houston, TX, 1987 (paper 224).
[15] A. Nagao, S. Kuramoto, K. Ichitani, M. Kanno, Visualization of hydrogen transport in high strength steels affected by stress fields and hydrogen trapping, Scripta Mater. 45 (2001) 1227–1232.
[16] J. Ovejero-García, Hydrogen microprint technique in the study of hydrogen in steels, J. Mater. Sci. 20 (1985) 2623–2629.
[17] H. Saito, K. Miyazawa, Y. Ishida, Tritium transmission electron-microscopic autoradiography of hydrogen trapping sites at interfaces in an austenitic stainless steel Sus316L, J. Jpn. Inst. Met. 55 (1991) 366–375.
[18] T. Asaoka, G. Lapasset, M. Aucouturier, P. Lacombe, Observation of hydrogen trapping in Fe-0.15 wt% Ti alloy by high resolution autoradiography, Corrosion 34 (1978) 39–47.
[19] N. Eliaz, D. Eliezer, E. Abramov, D. Zander, U. Köster, Hydrogen evolution from Zr-based amorphous and quasicrystalline alloys, J. Alloy Compd. 305 (2000) 272–281.
[20] A. Benninghoven, F.G. Rüdenauer, H.W. Werner, Secondary Ion Mass Spectrometry: Basic Concepts, Instrumental Aspects, Applications, and Trends, Wiley, New York, 1987.
[21] K. Takai, J. Seki, Y. Homma, Observation of trapping sites of hydrogen and deuterium in high-strength steels by using secondary ion mass spectrometry, Mater. Trans. JIM 36 (1995) 1134–1139.
[22] K. Takai, Y. Homma, K. Izutsu, M. Nagumo, Identification of trapping sites in high-strength steels by secondary ion mass spectrometry for thermally desorbed hydrogen, J. Jpn. Inst. Met. 60 (1996) 1155–1162.
[23] K. Takai, Y. Chiba, K. Noguchi, A. Nozue, Visualization of the hydrogen desorption process from ferrite, pearlite, and graphite by secondary ion mass spectrometry, Metall. Mater. Trans. A 33 (2002) 2659–2665.
[24] A.M. Brass, J. Chene, A. Boutry-Forveille, Measurements of deuterium and tritium concentration enhancement at the crack tip of high strength steels, Corros. Sci. 38 (1996) 569–585.
[25] J. Chene, F. Lecoester, A.M. Brass, D. Noel, SIMS analysis of deuterium diffusion in Alloy 600: The correlation between fracture mode and deuterium concentration profile, Corros. Sci. 40 (1998) 49–60.
[26] V.S. Sastri, D.B. McDonnell, Analysis of surface hydrogen in high-strength steels, Can. Metall. Quart. 34 (1995) 37–41.
[27] Scott X. Mao, M. Li, Mechanics and thermodynamics on the stress and hydrogen interaction in crack tip stress corrosion: experiment and theory, J. Mech. Phys. Solid 46 (1998) 1125–1137.
[28] V.I. Shvachko, Studies using negative secondary ion mass spectrometry: hydrogen on iron surface, Surf. Sci. 411 (1998) L882–L887.
[29] QQ-P-416, Plating, cadmium (electrodeposited), Federal Specification, 1995.
[30] W. Paatsch, V.-D. Hodoroaba, Hydrogen embrittlement in coating technology – measurement and testing, Plat. Surf. Finish. 89 (2002) 57–60.